Mean proton and α-particle reduced widths of the Porter-Thomas distribution and astrophysical applications

I. Pogrebnyak, C. Howard, C. Iliadis, R. Longland, and G. E. Mitchell

Phys. Rev. C **88**, 015808 — Published 31 July 2013

DOI: 10.1103/PhysRevC.88.015808

Mean proton and α-particle reduced widths of the Porter-Thomas distribution and astrophysical applications

I. Pogrebnyak,[1] C. Howard,[1,2] C. Iliadis,[1,2] R. Longland,[3,4] and G.E. Mitchell[2,5]

[1]*Department of Physics and Astronomy, University of North Carolina, Chapel Hill, North Carolina, 27599-3255, USA*

[2]*Triangle Universities Nuclear Laboratory, Durham, North Carolina 27708-0308, USA*

[3]*Departament de Física i Enginyeria Nuclear, EUETIB, Universitat Politecnica de Catalunya, c/ Comte d'Urgell 187, E-08036 Barcelona, Spain*

[4]*Institut d'Estudis Espacials de Catalunya (IEEC), Ed. Nexus-201, C/ Gran Capitá 2-4, E-08034 Barcelona, Spain*

[5]*Department of Physics, North Carolina State University, Raleigh, North Carolina, 27695, USA*

Abstract

The Porter-Thomas distribution is a key prediction of the Gaussian orthogonal ensemble in random matrix theory. It is routinely used to provide a measure for the number of levels that are missing in a given resonance analysis. The Porter-Thomas distribution is also of crucial importance for estimates of thermonuclear reaction rates where the contributions of certain unobserved resonances to the total reaction rate need to be taken into account. In order to estimate such contributions by randomly sampling over the Porter-Thomas distribution, the mean value of the reduced width must be known. We present mean reduced width values for protons and α-particles of compound nuclei in the $A = 28 - 67$ mass range. The values are extracted from charged-particle elastic scattering and reaction data that were measured at the Triangle Universities Nuclear Laboratory over several decades. Our new values differ significantly from those previously reported that were based on a preliminary analysis of a smaller data set. As an example for the application of our results, we present new thermonuclear rates for the ^{40}Ca(α,γ)^{44}Ti reaction, which is important for ^{44}Ti production in core-collapse supernovae, and compare with previously reported results.

I. INTRODUCTION

The statistical theory of nuclear reactions assumes that the reduced width amplitude for formation or decay of an excited compound nucleus is a random variable, with many small contributions from different parts of configuration space. If the contributing nuclear matrix elements are random in magnitude and sign, then the reduced width amplitude is represented by a Gaussian probability density centered at zero, according to the central limit theorem of statistics. Consequently, the corresponding reduced width, i.e., the square of the amplitude, is described by a chi-squared probability density with one degree of freedom. The latter distribution was proposed by Porter and Thomas [1] in the 1950s and has been shown to be a key prediction of the Gaussian orthogonal ensemble in random matrix theory. The basic assumption is that energy levels in atomic nuclei at several MeV excitation energies represent chaotic systems [2]. This aspect of quantum chaos linking nuclear physics with other fields has attracted significant interest in the literature. For reviews, see Refs. [3, 4]. The validity of the Porter-Thomas distribution for neutron and charged-particle reduced widths has been well established over many decades of experimental and theoretical research, and claims to the contrary have always been debated extensively. For recent discussions, see, for example, Refs. [5–8]. In fact, the Porter-Thomas distribution is so successful that it is routinely used to provide a measure for the number of levels that are missing in a given resonance analysis.

The Porter-Thomas distribution is also of crucial importance for nuclear applications [9]. It has been shown recently to impact estimates of thermonuclear reaction rates [10] in situations where the contributions of unobserved resonances to the total reaction rate need to be taken into account. In particular, for estimating such reaction rate contributions by randomly sampling over the Porter-Thomas distribution, the mean value of the reduced width must be known. Unfortunately, the mean reduced width values are usually not reported in the literature. A first attempt of extracting this information from existing proton elastic scattering and (p,α) reaction data for application to nuclear astrophysics was reported in Ref. [10]. However, the data set analyzed in that work was relatively small, and therefore, those results should be considered only as preliminary. In the present work, we reanalyze a more extensive data set for A=28−67 target nuclei. Note that the mean reduced width is closely related to the strength function, which is a key ingredient for estimating the average cross section of a nuclear reaction.

The formalism and our method of analysis are described in Sec. II. Data selection and results are discussed in Secs. III and IV, respectively. As an example for the application of our results, we provide new thermonuclear rates for the ^{40}Ca(α,γ)^{44}Ti reaction in Sec. V. A summary of our results is given in Sec. VI.

II. FORMALISM

A. Porter-Thomas Distribution

The particle partial width for a given level λ and channel c is defined by [11]

$$\Gamma_{\lambda c} = 2\gamma_{\lambda c}^2 P_c = 2\frac{\hbar^2}{mR^2} P_c \theta_{\lambda c}^2 \tag{1}$$

with $m = m_0 m_1/(m_0 + m_1)$ the reduced mass of the interacting species 0 and 1, P_c the penetration factor, $\gamma_{\lambda c}^2$ the reduced width, $\theta_{\lambda c}^2$ the dimensionless reduced width, $\theta_{\lambda c}$ the reduced width amplitude, and $R = R_0(A_0^{1/3} + A_1^{1/3})$ fm the channel radius, where A_i denotes (integer) mass numbers of the interacting nuclei.

The distribution of reduced particle widths for a single channel in a given nucleus of mass A and charge Z, given spin, parity, orbital angular momentum and channel spin, for levels above an excitation energy of several MeV is represented by the Porter-Thomas distribution [1],

$$f(y) = \frac{1}{\sqrt{2\pi y}} e^{-\frac{y}{2}} \tag{2}$$

where $y \equiv \theta^2/\langle\theta^2\rangle$, and $\langle\theta^2\rangle$ denotes the mean value of the dimensionless reduced width. The above equation is equivalent to a chi-squared distribution with one degree of freedom. It implies that the reduced widths for a single reaction channel, i.e., for a given nucleus and set of quantum numbers, vary by several orders of magnitude, with a higher probability for smaller values of the reduced width. Until recently [10], this fundamental prediction of random matrix theory had been disregarded in nuclear astrophysics. It was shown in Refs. [12, 13] that a proper treatment of the contributions from unobserved resonances, based on the Porter-Thomas distribution, can change the estimated total thermonuclear reaction rate by orders of magnitude compared to previous predictions.

For randomly sampling reduced widths, e.g., in a Monte Carlo procedure to estimate reaction rates, Eq. (2) needs to be expressed explicitly in terms of the mean value $\langle\theta^2\rangle$, which

is equal to the variance of the Gaussian distribution for the reduced width amplitudes, by

$$g(\theta^2) = \frac{1}{\sqrt{2\pi\theta^2 \langle\theta^2\rangle}} e^{-\frac{\theta^2}{2\langle\theta^2\rangle}} \tag{3}$$

The mean value $\langle\theta^2\rangle$ for a single channel may vary with increasing excitation energy since the complexity of the compound levels will increase. Therefore, the quantity $\langle\theta^2\rangle$ represents the *local* mean value, appropriate for a given region of excitation energy. The dependence of the mean reduced width on excitation energy will be addressed in Sec. IV.

The mean reduced width is related to the *strength function* of channel c via $s_c^J \equiv \langle\gamma_{\lambda c}^2\rangle / D^J$, where D^J is the mean energy spacing for compound levels of spin J. The strength function is closely related to the transmission coefficient, which is a key ingredient for estimating average nuclear reaction cross sections [11, 14]. The parameter $\langle\theta^2\rangle$, or equivalently, $\langle\gamma^2\rangle$, is not predicted by random matrix theory, but can be obtained from the analysis of laboratory data (Sec. III). Furthermore, the strength function can be estimated by using suitable models of nuclear reactions (e.g., the optical model).

Notice that summing reduced widths over different channels will give rise to a probability distribution that is generally different from the Porter-Thomas form. For example, the probability density for reduced widths summed over channel spin in cases where there are *two* channel spins is given by a chi-squared probability density with *two* degrees of freedom, assuming the mean reduced widths to be the same for the two channel spins. Furthermore, if level sequences for *different* channels are combined to improve statistics, it generally can not be assumed that the combined sequence follows a Porter-Thomas distribution because the mean reduced widths of the sequences may be different.

B. Maximum Likelihood

Consider a sequence of observed dimensionless reduced widths, containing N_{obs} levels for a given parameter set $A, Z, J^\pi, \ell, s, \Delta E_x$. The data set has a minimum value of θ_{min}^2, caused by an experimental detection limit. The observed mean value of the reduced width is given by

$$\left\langle\theta^2\right\rangle_{obs} = \frac{1}{N_{obs}} \sum_{i=1}^{N_{obs}} \theta_i^2 \tag{4}$$

Two corrections need to be applied in order to deduce the actual mean, $\langle\theta^2\rangle$, from the observed mean: N_{obs} needs to be corrected for the fraction of missing levels with widths below

θ^2_{min}, and $\sum_i \theta_i^2$ has to be corrected for the fraction of missing strength. The corrections could in principle be found using Eq. (2), and $\langle\theta^2\rangle$ could then be determined from an iterative method. However, it is difficult to extract uncertainties from such a procedure. Following the method of Fröhner [15], we start with a truncated Porter-Thomas distribution,

$$h(\theta^2) = \begin{cases} 0 & , \theta^2 < \theta^2_{min} \\ \frac{1}{\mathrm{erfc}\left(\sqrt{\theta^2_{min}/2\langle\theta^2\rangle}\right)} \frac{e^{-\frac{\theta^2}{2\langle\theta^2\rangle}}}{\sqrt{2\pi\theta^2\langle\theta^2\rangle}} & , \theta^2 \geq \theta^2_{min} \end{cases} \tag{5}$$

where erfc denotes the complementary error function. The truncated Porter-Thomas distribution is normalized to unity between θ^2_{min} and infinity. The likelihood function for the mean value of the dimensionless reduced width is then given by

$$L(\langle\theta^2\rangle) = \prod_{i=1}^{N_{obs}} h(\theta_i^2) \tag{6}$$

The most likely value of $\langle\theta^2\rangle$ is found from the condition that the likelihood function attains its maximum value, L_{max}. Instead of maximizing Eq. (6), it is more convenient, but equivalent, in the parameter search to minimize the quantity $\mathcal{L}(\langle\theta^2\rangle) \equiv -2\log L(\langle\theta^2\rangle)$. From Eqs. (5) and (6), we find

$$\begin{aligned} \mathcal{L}(\langle\theta^2\rangle) = 2N_{obs} \log \left[\mathrm{erfc}\sqrt{\theta^2_{min}/2\,\langle\theta^2\rangle}\right] \\ + \sum_{i=1}^{N_{obs}} \left[\frac{\theta_i^2}{\langle\theta^2\rangle} + \log\left(2\pi\theta_i^2\,\langle\theta^2\rangle\right)\right] \end{aligned} \tag{7}$$

which can be further simplified for efficient numerical minimization.

C. Uncertainties and Test of Method

In order to estimate $\langle\theta^2\rangle$ from Eq. (7), we used `ROOT's TMinuit` class that implements the `Minuit` function minimization [16]. We adopt the standard deviation of the mean reduced width for the uncertainty. For a Porter-Thomas distribution, it is given by

$$\sigma_{\langle\theta^2\rangle} = \langle\theta^2\rangle \sqrt{\frac{2}{N_{obs}}} \tag{8}$$

where N_{obs} is the number of reduced width values in the level sequence. It can be shown [17] that this choice corresponds to a decrease in $\log L_{max}$ by 1/2,

$$\log L\left(\langle\theta^2\rangle \pm \sigma_{\langle\theta^2\rangle}\right) = \log L_{max} - \frac{1}{2} \tag{9}$$

Monte Carlo simulations have been performed to verify our analysis procedure. Synthetic data sequences are randomly sampled according to Eq. (3) for a fixed mean reduced width value of 0.01, and then analyzed according to Eqs. (5)–(8) in order to extract values of $\langle\theta^2\rangle$ and $\sigma_{\langle\theta^2\rangle}$ from each sequence. Examples are displayed in Fig. 1 for conditions similar to those of the experimental data sequences (Sec. III). Each synthetic data sequence originally contained 50 reduced width values (without cutoff, see below).

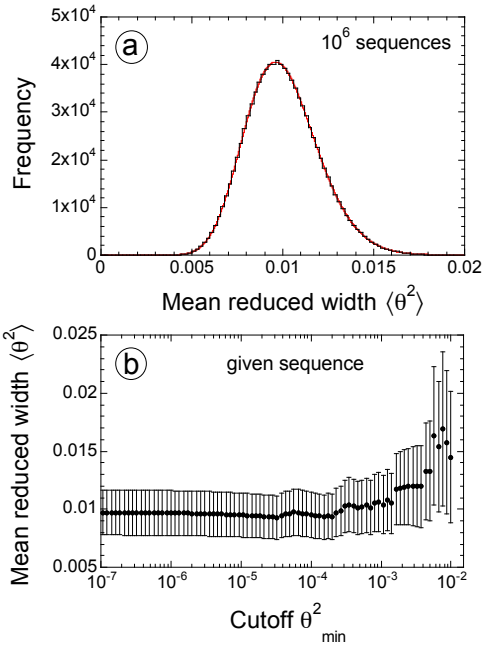

FIG. 1. (Color online) Test of analysis procedure using synthetic data sequences. Each sequence contains originally 50 reduced width values (without cutoff), randomly sampled according to Eq. (3), with a mean reduced width of 0.01. (Top) extracted mean reduced width versus number of sequences; the total number of sequences sampled amounts to 10^6; the red curve shows the probability density given by a chi-squared distribution with $N = 50$ degrees of freedom; see text. (Bottom) cutoff value θ^2_{min} versus extracted mean reduced width for a given data sequence; notice how the uncertainties increase with a higher cutoff value and a smaller number of levels available in the analysis.

The top panel shows the number of sequences versus the extracted mean reduced width values, where the total number of sequences amounts to 10^6. The mean value and standard

deviation of the displayed distribution are $\langle\theta^2\rangle$=0.0100 and $\sigma_{\langle\theta^2\rangle}$=0.0020, respectively, and are in agreement with the uncertainty estimate from Eq. (8). The bottom panel displays the dependence of the extracted mean reduced width, $\langle\theta^2\rangle$, on the minimum reduced width, θ^2_{min}, or cutoff, for a single representative synthetic sequence. The mean reduced width value for the sequence is $\langle\theta^2\rangle = 0.0097$. This sequence, without the cutoff, contained 50 reduced width values, and was progressively truncated, with all reduced width values below the cutoff removed. A number of observations can be made: (i) the extracted mean reduced width values are consistent for different values of θ^2_{min} and agree within uncertainties with the originally assumed fixed value 0.01 that was employed to randomly sample this sequence in the first place; (ii) the uncertainty, $\sigma_{\langle\theta^2\rangle}$, increases as the cutoff value, θ^2_{min}, increases in magnitude and fewer number of levels are available in the analysis. The results demonstrate that the extracted mean reduced width values are stable when the cutoff is allowed to vary.

Simulations similar to those shown in Fig. 1 have been performed for sequence sizes of 10, 100, and 300. In each case we find results consistent with those described above.

D. Probability density function of mean reduced width

For the estimation of thermonuclear reaction rates using a Monte Carlo-based procedure [10], reduced widths for unobserved resonances can be randomly sampled according to a Porter-Thomas distribution if the mean reduced width is known, as discussed in Sec. I. Here we not only present mean reduced widths for given compound nuclei, but also extract associated uncertainties. In addition to the random sampling of a reduced width value, this allows for the random sampling of the *mean* reduced width. However, this requires the identification of a suitable probability density function that corresponds to the results presented here. This probability density is discussed below.

Suppose a sample data set containing N values is generated by randomly sampling a Porter-Thomas distribution (Eq. 3). It can be shown that in this case the maximum likelihood estimator of the mean reduced width is given by $\langle\hat{\theta^2}\rangle = (1/N)\sum_{i=1}^{N}\theta_i^2$. In other words, the quantity $\langle\theta^2\rangle\, N$ is also a random variable and depends on the sum of N independent squares of θ_i, where the latter quantity is distributed according to a Gaussian with a variance of $\langle\theta^2\rangle$ (Secs. I and II A). Consequently, the probability density of $\langle\theta^2\rangle\, N$ is given by a

chi-squared distribution with N degrees of freedom

$$u(x) = \left(\frac{x}{2p}\right)^{\frac{N}{2}} \frac{e^{-\frac{x}{2p}}}{x\Gamma(N/2)} \tag{10}$$

where $x = \theta^2$, $p = \langle\theta^2\rangle / N$, and Γ denotes the Gamma function. The mean value and variance of the above distribution are given by

$$E[x] = Np = \langle\theta^2\rangle \quad , \qquad V[x] = 2Np^2 = \frac{2}{N}\langle\theta^2\rangle^2 \tag{11}$$

$$p = \frac{V[x]}{2E[x]} = \frac{\langle\theta^2\rangle}{N} \quad , \qquad N = \frac{2E[x]^2}{V[x]} \quad , \tag{12}$$

As an example, consider again Fig. 1 (top), where we had obtained the values of $E[x] = \langle\theta^2\rangle$=0.0100 and $\sqrt{V[x]} = \sigma_{\langle\theta^2\rangle}$=0.0020 for the distribution shown. From these results we find with Eq. (12) the values $p = 0.00020$ and $N = 50.0$, which were used to generate the red curve in Fig. 1 (top) according to Eq. 10. The agreement between the probability density (red curve) and the distribution resulting from the synthetic data sequences is apparent. To summarize, a mean reduced width and uncertainty reported below for a given level sequence can be used to compute the parameters p and N, which determine the probability density function of $\langle\theta^2\rangle$ according to Eq. 10.

III. DATA BASE

The difficulties in estimating the quantity $\langle\theta^2\rangle$ by applying Eq. (5) to measured data are readily apparent. First, for a fixed $\langle\theta^2\rangle$ value, the above expression applies only to a sequence of levels appropriate for a single channel, i.e., for a given nucleus (A, Z); given values for spin-parity (J^π), orbital angular momentum (ℓ), and channel spin (s); and a given range of excitation energy (ΔE_x). Therefore, a rather large body of data is required such that the sets of fixed A, Z, J^π, ℓ, s, and E_x values contain a statistically significant number of levels. Second, the nuclear level sequence for a fixed data set should ideally be complete, i.e., all levels should have been observed. In reality, each measurement is subject to a detection limit prohibiting the observation of very weak resonances. Therefore, corrections for the fraction of missing levels must be applied to the data (Sec. II B). Third, the data need to be of high quality so that the resonance properties (partial width, spin, parity and orbital angular momentum) can be extracted reliably. Obviously, a few states with wrongly assigned spin

and parity in a sequence of a small number of nuclear levels may have a large impact on the derived mean reduced width value. Fourth, the Porter-Thomas distribution only applies to compound levels that are "statistical" in nature, in the sense that a given reduced width has many small contributions from different parts of configuration space (Sec. II A). Therefore, one may not assume that reduced widths that result from a few large contributions follow a Porter-Thomas distribution. Examples include isobaric analog states in the case of proton reduced widths, and α-particle cluster states for α-particle reduced widths. The presence of such levels may enhance the reduced widths of neighboring states that share the same J^π value and thereby distort the reduced width distribution. Such "non-statistical" levels need to be removed carefully from a level sequence before Eq. (5) can be applied.

The data analyzed here were measured at the 3-MeV Van de Graaff accelerator laboratory over a period of 30 years, which was part of the Triangle Universities Nuclear Laboratory (TUNL) until the machine was decommissioned in 2004. All of the data are available online [18]. A number of aspects are noteworthy regarding this unique data set: (i) the proton elastic scattering and (p,α) reaction experiments were performed at bombarding energies well below the top of Coulomb barrier, where the strong Coulomb effect produces sharp, narrow resonances and permits easy identification of orbital angular momenta; (ii) the energy resolution of the experimental system was superb ($\approx 200-450$ eV for thin solid transmission targets), allowing for the observation of weak and closely spaced nuclear resonances with widths down to $\approx$5 eV; (iii) the data set spans target nuclei in the mass range of A=28$-$67, and therefore, has a significant overlap with target nuclei of astrophysical interest; and (iv) the elastic scattering data were analyzed using the same R-matrix code (MULTI [19], and subsequent versions) and similar analysis procedures were applied. For more information, the reader is referred to Refs. [20, 21].

Only part of the data analyzed here were used by Longland and collaborators [10] to extract mean reduced width values. However, as pointed out in Ref. [10], the data set was small and, as a result, the data for different compound nuclei, spins, parities and orbital angular momenta had to be combined into a single set in order to analyze a statistically significant number of nuclear levels. For the reasons mentioned above, those results should be regarded only as preliminary.

In the present work, a much larger data set is analyzed. Our strategy can be summarized as follows. First, we compiled all of the proton and α-particle *partial* widths, Γ_i. Second,

the partial widths were converted to dimensionless reduced widths, θ_i^2, by using Eq. (1). For the radius parameter we employ the common value of $R_0 = 1.25$ fm. Third, dimensionless reduced widths were grouped into level sequences according to fixed A, Z, J^π, ℓ, s, and E_x values. Fourth, all sequences were inspected for "non-statistical" states. If positively identified (see below), such states were removed from the data set. At this stage all α-particle (proton) level sequences that contained less than 10 (15) states were deemed of poor statistics and were disregarded. Finally, all remaining level sequences were analyzed by using the formalism described in Sec. II C.

Non-statistical levels with large reduced widths frequently manifest themselves in a level sequence as anomalous large steps in the cumulative reduced width distribution. Further evidence is required to support this conclusion. For example, isobaric analog states in a daughter nucleus should correspond to levels of same spin and parity in the parent nucleus, with an expected difference in excitation energy (mainly caused by the Coulomb interaction) and related single-nucleon spectroscopic factors [20]. However, it is not always straightforward to identify the presence of analog states in a given level sequence, especially at higher excitation energies where the level density becomes larger and less experimental information is available for parent states. We made the following assumptions in the data treatment: (i) if a given level sequence exhibits no anomalous steps in the cumulative reduced width distribution, then either no "non-statistical" levels are present, or such levels are too weak to impact the value of $\langle\theta^2\rangle$ significantly; consequently, no attempt was made to remove any states from that level sequence; (ii) if the cumulative reduced width distribution exhibits distinct steps, and the steps correspond to known "non-statistical" levels (i.e., analog states in the proton data, or α-cluster states in the α-particle data), then these levels were removed from the level sequence; (iii) if the cumulative reduced width distribution exhibits distinct steps, but not enough information was available for a positive identification as "non-statistical" levels, we removed the entire level sequence from further analysis.

Information on the data analyzed in the present work, including references to the original works that measured the elastic scattering and nuclear reaction data, is provided in Tabs. I, II and III. The columns list for each compound nucleus (shown in boldface) the level spin and parity (J^π), orbital angular momentum, channel spin (for protons only), excitation energy range ($E_{x_i} - E_{x_f}$), and, for each level sequence, the number of observed levels (N_{obs}), the minimum reduced width (θ^2_{min}), and the mean reduced width value ($\langle\theta^2\rangle$) obtained in

the present work. The results for α-particles and protons are discussed separately below.

TABLE I. Summary of individual level sequences for α-particle reduced widths in A=28−40 nuclei analyzed in the present work.[a]

J^π	ℓ	E_{x_i}–E_{x_f} (MeV)	$N_{\rm obs}$	$\theta^2_{\rm min}$	$\langle\theta^2_\alpha\rangle$
^{27}Al + p → $^{\mathbf{28}}$**Si** (Q = 11.585 MeV); Ref. [22]					
2^+	2	12.727 – 14.494	14	0.00092	0.030(11)
4^+	4	12.856 – 14.328	11	0.00061	0.032(14)
^{31}P + p → $^{\mathbf{32}}$**S** (Q = 8.864 MeV); Ref. [23]					
1^-	1	10.698 – 12.738	17	0.000082	0.0216(74)
2^+	2	10.293 – 12.595	18	0.00011	0.0164(55)
3^-	3	11.804 – 12.661	10	0.0022	0.0111(50)
^{35}Cl + p → $^{\mathbf{36}}$**Ar** (Q = 8.507 MeV); Ref. [24]					
1^-	1	10.172 – 12.360	37	0.00022	0.0224(52)
2^+	2	10.700 – 12.305	24	0.00043	0.0178(51)
^{39}K + p → $^{\mathbf{40}}$**Ca** (Q = 8.328 MeV); Ref. [25, 26]					
1^-	1	10.362 – 12.245	50	0.000053	0.0208(42)
2^+	2	10.657 – 12.226	47	0.00012	0.0136(28)
3^-	3	10.333 – 12.200	21	0.00041	0.0110(34)
4^+	4	11.128 – 12.243	25	0.00024	0.0111(31)

[a] References for each reaction indicate original source of experimental partial widths.

TABLE II. Summary of individual level sequences for proton reduced widths in A=34−49 nuclei analyzed in the present work.[a]

J^π	ℓ	s	E_{x_i}–E_{x_f} (MeV)	$N_{\rm obs}$	$\theta^2_{\rm min}$	$\langle\theta^2_\alpha\rangle$
^{33}S + p → $^{\mathbf{34}}$**Cl** (Q = 5.143 MeV); Ref. [27]						
2^+	0	2	6.851 – 8.697	17	0.00011	0.00117(40)
^{35}Cl + p → $^{\mathbf{36}}$**Ar** (Q = 8.507 MeV); Ref. [24]						
1^-	1	1	9.982 – 12.296	20	0.000029	0.0067(21)
1^-	1	2	9.982 – 12.274	37	0.0000082	0.0055(13)
2^+	2	2	10.700 – 11.861	15	0.00029	0.0031(11)
^{39}K + p → $^{\mathbf{40}}$**Ca** (Q = 8.328 MeV); Ref. [25, 26]						
0^+	2	2	10.541 – 11.962	15	0.00022	0.0053(19)
1^+	2	2	10.722 – 12.237	21	0.00042	0.00202(62)
2^+	0	2	10.657 – 12.226	37	0.0000031	0.00050(12)
^{42}Ca + p → $^{\mathbf{43}}$**Sc** (Q = 4.930 MeV); Ref. [28]						
$1/2^+$	0	1/2	6.408 – 7.831	37	0.000032	0.00083(19)
^{44}Ca + p → $^{\mathbf{45}}$**Sc** (Q = 6.888 MeV); Ref. [28–30]						
$1/2^+$	0	1/2	8.528 – 10.515	198	0.0000061	0.000238(24)
$3/2^+$	2	1/2	9.334 – 10.516	238	0.000023	0.000192(18)
$3/2^-$	1	1/2	8.894 – 10.497	182	0.000010	0.000096(10)
$5/2^+$	2	1/2	9.336 – 10.518	144	0.000012	0.000156(18)
$5/2^-$	3	1/2	9.334 – 10.332	72	0.000088	0.000489(81)
^{46}Ti + p → $^{\mathbf{47}}$**V** (Q = 5.168 MeV); Ref. [31]						
$1/2^+$	0	1/2	7.211 – 8.170	21	0.000052	0.00093(29)
$5/2^+$	2	1/2	7.636 – 8.038	16	0.000085	0.00061(21)
^{48}Ti + p → $^{\mathbf{49}}$**V** (Q = 6.758 MeV); Ref. [31, 32]						
$1/2^+$	0	1/2	8.700 – 10.536	170	0.0000081	0.000519(56)
$1/2^-$	1	1/2	8.793 – 10.536	147	0.000011	0.000446(52)
$3/2^+$	2	1/2	9.391 – 10.519	146	0.000025	0.000223(26)
$5/2^+$	2	1/2	9.385 – 10.538	190	0.000024	0.000228(23)

[a] References for each reaction indicate original source of experimental partial widths.

TABLE III. Summary of individual level sequences for proton reduced widths in A=51−67 nuclei analyzed in the present work.[a]

J^π	ℓ	s	E_{x_i}–E_{x_f} (MeV)	$N_{\rm obs}$	$\theta^2_{\rm min}$	$\langle\theta^2_\alpha\rangle$
^{50}Cr + p → $^{\mathbf{51}}$**Mn** (Q = 5.271 MeV); Ref. [33]						
$1/2^+$	0	1/2	7.050 – 8.689	25	0.000082	0.00318(90)
^{52}Cr + p → $^{\mathbf{53}}$**Mn** (Q = 6.560 MeV); Ref. [34]						
$1/2^+$	0	1/2	8.656 – 9.961	55	0.000041	0.00155(30)
$1/2^-$	1	1/2	8.640 – 9.949	44	0.000078	0.00081(17)
$3/2^+$	2	1/2	8.866 – 9.963	21	0.000032	0.00071(22)
$5/2^+$	2	1/2	8.847 – 9.942	86	0.000036	0.00071(11)
^{54}Cr + p → $^{\mathbf{55}}$**Mn** (Q = 8.067 MeV); Ref. [35]						
$1/2^+$	0	1/2	10.071 – 10.703	52	0.00010	0.00058(11)
^{54}Fe + p → $^{\mathbf{55}}$**Co** (Q = 5.064 MeV); Ref. [36]						
$3/2^-$	1	1/2	8.291 – 9.491	29	0.000045	0.00096(25)
^{56}Fe + p → $^{\mathbf{57}}$**Co** (Q = 6.028 MeV); Ref. [37]						
$1/2^+$	0	1/2	9.094 – 9.958	56	0.000036	0.00105(20)
$3/2^+$	2	1/2	9.095 – 9.919	29	0.000073	0.00093(24)
$3/2^-$	1	1/2	9.078 – 9.951	40	0.000017	0.000147(33)
$5/2^+$	2	1/2	9.098 – 9.959	80	0.000048	0.00072(11)
^{60}Ni + p → $^{\mathbf{61}}$**Cu** (Q = 4.801 MeV); Ref. [36]						
$1/2^+$	0	1/2	7.744 – 8.175	21	0.000051	0.00086(27)
^{64}Zn + p → $^{\mathbf{65}}$**Ga** (Q = 3.943 MeV); Ref. [38]						
$1/2^+$	0	1/2	6.465 – 7.127	32	0.00030	0.00097(24)
^{66}Zn + p → $^{\mathbf{67}}$**Ga** (Q = 5.269 MeV); Ref. [38]						
$1/2^+$	0	1/2	7.840 – 8.479	102	0.000068	0.000344(48)

[a] References for each reaction indicate original source of experimental partial widths.

IV. RESULTS

A. Mean α-particle reduced widths

In total, mean α-particle reduced widths could be extracted for 11 level sequences. The data analyzed correspond to compound nuclei in the $A = 28 - 40$ range. For each sequence the minimum observed width, θ^2_{min}, is far smaller than the extracted mean value. The largest sequence contains 50 levels (for 1^- states in ^{40}Ca). Results are displayed in Fig. 2. Different colors correspond to different J^π values. The numbers next to the data points indicate the average excitation energy of each sequence.

It is apparent that the dependence of $\langle\theta^2_\alpha\rangle$ on mass number, A, is weak, although the values for $A = 28$ seem slightly high. However, it must be noted that those two level sequences are located about 2 MeV higher in the compound nucleus compared to the other displayed sequences. Furthermore, at each mass number, A, the uncertainties of the data points for different J^π values overlap. The only exception is the 1^- level sequence in $A = 40$, although the relatively large uncertainties preclude firmer conclusions. It should be emphasized that the results displayed in Fig. 2 confirm our assumption that strong α-cluster states are absent in the level sequences analyzed here, since otherwise the mean reduced width values for different masses and spin-parities would not be in such good agreement.

Because of the weak dependence of $\langle\theta^2_\alpha\rangle$ on both A and J^π, we combined level sequences in order to improve statistics. The results are displayed in Fig. 3. The top panel shows the mean reduced widths versus mass number, A, when all sequences regardless of differences in J^π are combined. The bottom panel displays $\langle\theta^2_\alpha\rangle$ versus J^π when all sequences regardless of differences in A are combined. The number next to a data point corresponds again to the average excitation energy of the combined sequence. In both panels, the data are in reasonable agreement with the assumption that $\langle\theta^2_\alpha\rangle$ is nearly independent of A and J^π. If we combine all 11 level sequences into one set, a value of $\langle\theta^2_\alpha\rangle = 0.018\pm0.002$ is found. These boundaries are shown as horizontal lines in Fig. 3. Note that this value is about a factor of 2 higher than the result reported previously ($\langle\theta^2_\alpha\rangle$=0.010 from the preliminary study of Ref. [10]), which was based on a subset of the full (p,α) data set analyzed here.

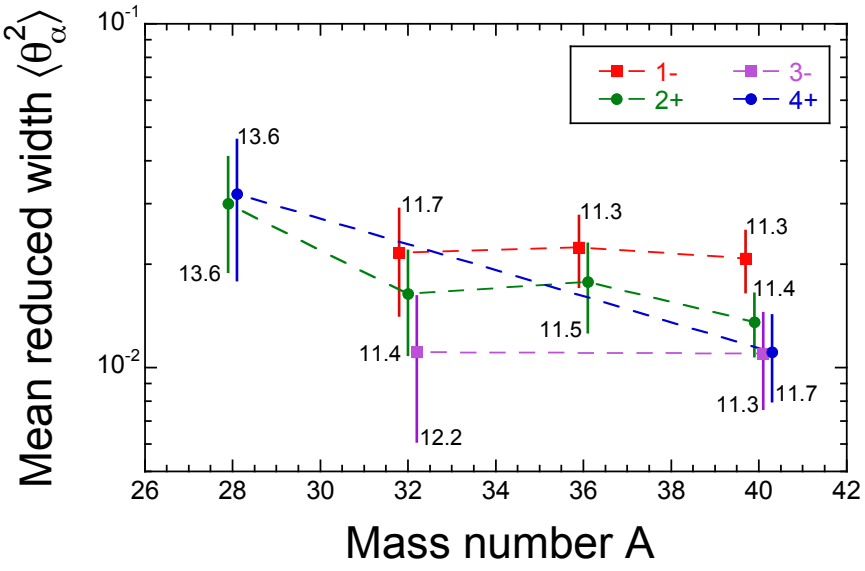

FIG. 2. (Color online) Mean α-particle reduced width versus mass number of the compound nucleus. All values displayed, also listed in the last column of Tab. I, have been extracted from (p,α) reaction data using the formalism presented in Sec. II. Data points of different color signify different J^π values. Data points corresponding to the same mass number but different J^π value are slightly displaced horizontally in order to improve the presentation. Values next to a data point indicate the mean excitation energy of the analyzed level sequence. Solid or dashed lines connect values belonging to the same spin-parity and are to guide the eye only.

B. Mean proton reduced widths

Significantly more data are available for proton reduced widths compared to α-particle reduced widths. In total, mean proton reduced widths could be extracted for 33 level sequences. The data analyzed correspond to compound nuclei in the $A = 34 - 67$ range. Again, for each sequence the minimum observed width, θ^2_{min}, is far smaller than the extracted mean value. The largest sequence contains 238 levels (for $3/2^+$ states in ^{45}Sc). Results are displayed in Fig. 4. Different colors correspond to different spins, while full circles (squares) indicate positive (negative) parity.

As is apparent from Tabs. II and III, the number of levels contained in each analyzed sequence is on average much higher compared to the α-particle data, resulting in smaller uncertainties of the derived $\langle\theta_p^2\rangle$ values. Furthermore, comparison of Figs. 2 and 4 shows

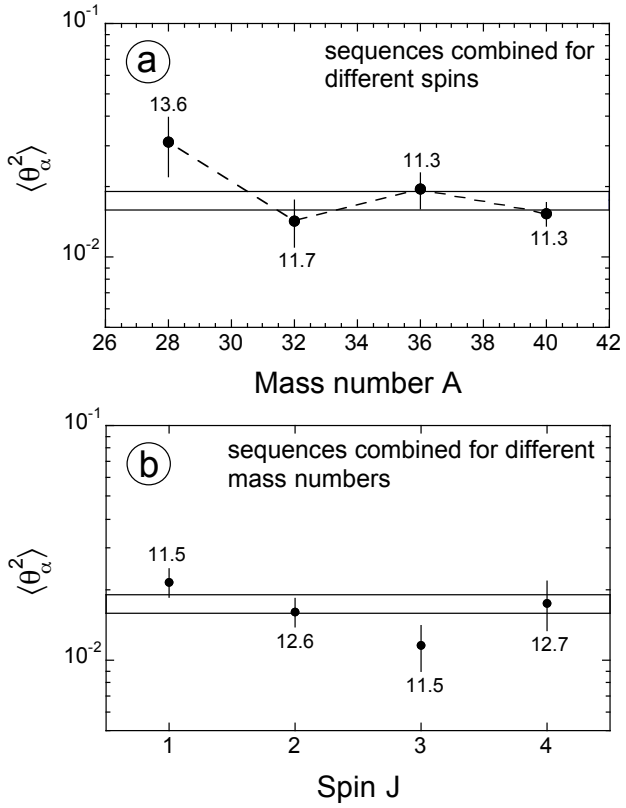

FIG. 3. Mean α-particle reduced width versus (top) mass number of the compound nucleus, (bottom) spin of the compound nucleus. In the top panel, all level sequences for a given mass number, A, are combined in the analysis, regardless of differences in spin and parity (unlike the values shown in Fig. 2). In the bottom panel, all level sequences for a given spin, J, are combined in the analysis, regardless of differences in mass number. Numbers next to a data point indicate the mean excitation energy of the analyzed level sequence. In both panels the average reduced width, $\langle\theta_\alpha^2\rangle = 0.018 \pm 0.002$, that is obtained when all level sequences, regardless of spin, parity, or mass number, are combined, is indicated by the two horizontal lines.

that there is significant scatter in the proton mean reduced widths for different mass numbers and J^π values. For a given spin J, the $\langle\theta_p^2\rangle$ values scatter over up to an order of magnitude, depending on mass number. For $A \leq 40$ the mean reduced proton widths are higher, on average, compared to the $A > 40$ range. No other systematic trends can be identified easily.

The results displayed in Fig. 4 are important because they facilitate an improved random sampling of thermonuclear reaction rates: instead of using one *global* mean reduced proton width value for all mass numbers and spin-parities ($\langle\theta_p^2\rangle$=0.0045 reported in the preliminary study of Ref. [10]), the results of the present work allow for the first time to employ *local* values (see Fig. 4; Tabs. II and III) in the random sampling.

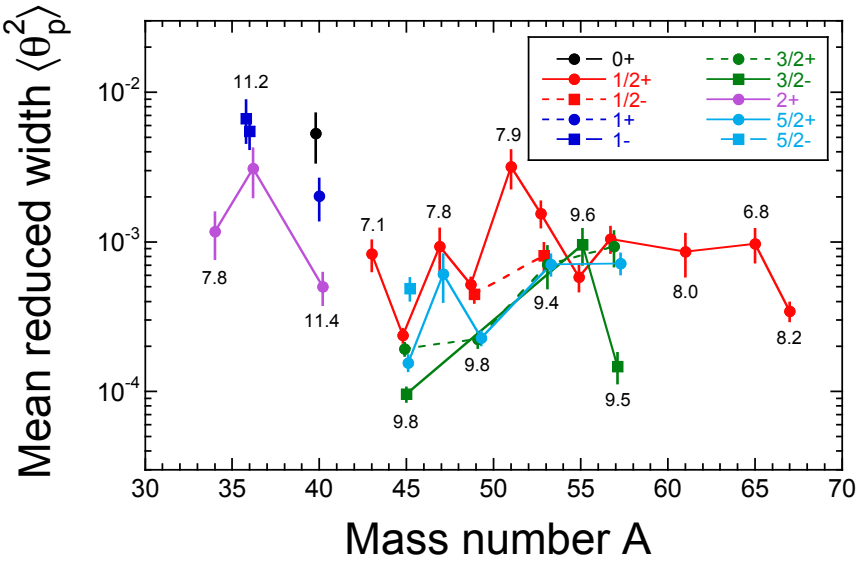

FIG. 4. (Color online) Mean proton reduced width versus mass number of the compound nucleus. All values displayed, also listed in the last column of Tabs. II and III, have been extracted from proton elastic scattering data using the formalism presented in Sec. II. Data points of different color signify different spins. Data points corresponding to the same mass number but different J^π value are slightly displaced horizontally in order to improve the presentation. Numbers below or above a group of data points indicate the mean excitation energy of all analyzed level sequences for that particular mass number. Solid or dashed lines connect values belonging to the same spin-parity and are to guide the eye only.

The numbers below or above a group of data points in Fig. 4 indicate the mean excitation energy of all analyzed level sequences for that particular mass number. The mean excitation energies, depending on the level sequence, vary between 6.8 MeV and 11.4 MeV. In order to investigate how much of the scatter in the displayed $\langle\theta_p^2\rangle$ values is caused by differences in the excitation energy, we considered the three level sequences with the highest statistics ($1/2^+$ and $3/2^+$ in ^{45}Sc, $1/2^+$ in ^{49}V; see Tab. II). Each of these was divided into 5 subsequences

that were individually analyzed using the procedure described in Sec. II. The results are displayed in Fig. 5, showing the mean reduced proton width versus the mean excitation energy of the subsequence. The numbers next to the data points indicate the total number of levels contained in each subsequence. It is apparent that $\langle\theta_p^2\rangle$ varies by a relatively small amount over an excitation energy range of ≈ 1.6 MeV. Thus we conclude that most of the scatter of $\langle\theta_p^2\rangle$ values shown in Fig. 4 is not caused by differences in excitation energy, but by the nuclear structure of the compound nucleus under consideration.

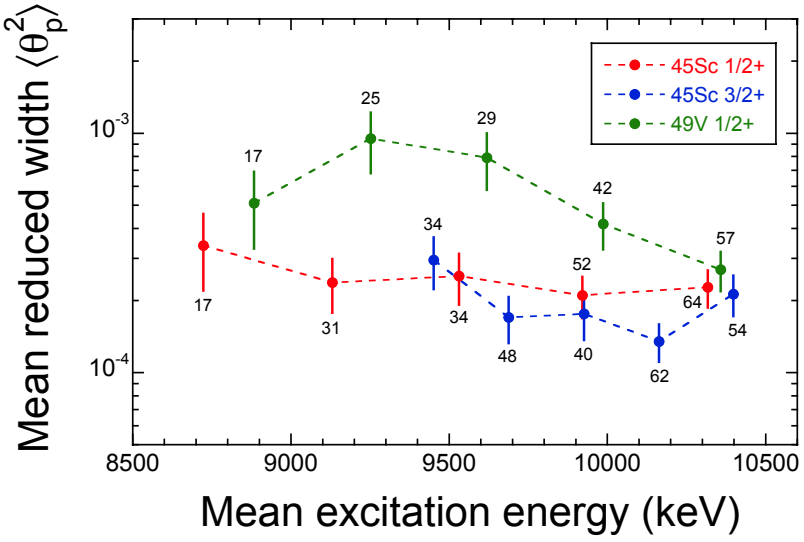

FIG. 5. (Color online) Mean proton reduced width versus mean excitation energy of subsequences (see text). The results are obtained by dividing the level sequences with the highest statistics ($1/2^+$ and $3/2^+$ in ^{45}Sc, $1/2^+$ in ^{49}V; Tab. II) into subsequences. Dotted lines are to guide the eye only. The numbers next to the data points indicate the total number of states contained in the subsequence. No strong systematic variation of the $\langle\theta_p^2\rangle$ values is apparent.

V. APPLICATION TO ^{40}CA(α,γ)^{44}TI THERMONUCLEAR RATES

In order to demonstrate the implications of our results, we calculate new thermonuclear rates for the ^{40}Ca(α,γ)^{44}Ti reaction ($Q_{\alpha\gamma} = 5127$ keV) that is responsible for the production of ^{44}Ti during the α-rich freeze out in core-collapse supernovae. The radioactive decay of ^{44}Ti is of paramount importance for core-collapse supernova light curves, γ-ray astronomy,

and isotopic anomalies measured in presolar grains (Refs. [39–41], and references therein). The important stellar temperature range for this reaction amounts to $T \approx 1 - 5$ GK.

The total rate is determined by observed and unobserved resonances. For the observed resonances, we adopt resonance energies and strengths from Refs. [42–45]. In total, 32 observed resonances at energies of $E_r^{c.m.} = 2507 - 5259$ keV are taken into account. In addition, 11 natural parity states between the α-particle threshold and the lowest-lying observed resonance can contribute to the total rate [46]. The compound nucleus ^{44}Ti exhibits a strong α-cluster structure, which was investigated in several works using α-particle transfer experiments. Sizable experimental spectroscopic factors are reported in Refs. [47, 48] (and references therein) for the unobserved resonances corresponding to levels near the α-particle threshold. We chose this example because, interestingly, there is a resonance at $E_r^{c.m.} = 2373$ keV ($E_x = 7500$ keV, $J^\pi = 1^-$ [46]), that has not been observed in any of the α-particle transfer studies. Since this level does not exhibit an α-cluster structure and no experimental information is known about the α-particle spectroscopic factor, it can be assumed that the probability density function of its reduced width is given by a Porter-Thomas distribution (Sec. II). Details on the nuclear data input and our new rate calculation will be presented in a forthcoming publication. Below we will focus on the main results.

The new experimental ^{40}Ca(α,γ)^{44}Ti rates are calculated using the Monte Carlo procedure outlined in Longland et al. [10]. All uncertainties of resonance energies and strengths are taken into account in the random sampling. Furthermore, for the mean reduced α-particle width of the unobserved $E_r^{c.m.} = 2373$ keV resonance we adopt a value of $\langle\theta_\alpha^2\rangle = 0.022 \pm 0.003$ that is obtained by combining all 1^- level sequences shown in Tab. I, regardless of mass number (see also Fig. 3, bottom). The probability density of the mean reduced width, given by a chi-squared distribution, is obtained in a similar manner to the example discussed in Sec. II D. Monte Carlo based reaction rates are then derived from 50,000 rate samples. The results are displayed in Fig. 6, where for a better comparison all rates are normalized to the present recommended (median) Monte Carlo rate (i.e., the 0.50 quantile of the cumulative rate distribution).

The colored shading indicates the coverage probability in percent (see legend on right-hand side). For example, the area enclosed by the thick black lines (i.e., the high and low Monte Carlo rates) corresponds to a coverage probability of 68%, while the area enclosed by the the thin black lines contains a coverage probability of 95%. The green line is ob-

tained when assuming a maximum possible contribution of the unobserved $E_r^{c.m.} = 2373$ keV resonance (i.e., for an α-spectroscopic factor of unity) and represents the *upper limit* of the classical reaction rate[1]. As can be seen, the probability density distribution of the ^{40}Ca(α,γ)^{44}Ti reaction rate in the temperature range of $T = 1-3$ GK is concentrated around much smaller values compared to the classical upper limit, and therefore, the latter rates represent an unlikely estimate. In fact, the Monte Carlo rates (thick black lines; for a 68% coverage probability) that are obtained by randomly sampling using a Porter-Thomas distribution for this single unobserved resonance are smaller by up to a factor of $\approx$3 compared to the classical upper limit (green line).

As a comparison, the blue lines show the (classical) "upper limit", "complete rate", and "lower limit" from the recent study of Robertson et al. [45]. The large deviation near $T = 1$ GK, by almost one order of magnitude, is caused by the fact that none of the unobserved resonances were taken into account by Ref. [45]. Part of the deviation at the higher temperature end near $T = 5$ GK is explained by the fact that Ref. [45] took only a subset of the available directly measured data into account (in particular, excluding Ref. [44]). Our new rates, based partially on the results of the present work, may have a significant impact on the final ^{44}Ti yields in core-collapse supernovae.

VI. SUMMARY AND CONCLUSIONS

The Porter-Thomas distribution is of crucial importance for estimates of thermonuclear reaction rates in situations where the contributions of unobserved resonances to the total reaction rate need to be taken into account [10]. For estimating such contributions by randomly sampling over the Porter-Thomas distribution, the mean value of the reduced width must be known. We have presented here mean reduced width values for protons and α-particles of compound nuclei in the $A = 28 - 67$ mass range. The values are extracted from charged-particle elastic scattering and reaction data that were measured at TUNL over several decades. Our new values differ significantly from those reported previously [10] that were based on a preliminary analysis of a much smaller data set.

[1] The expression *classical reaction rate* refers to the result of the procedure that was commonly applied before the advent of Monte Carlo based reaction rates [10]. In order to avoid confusion, the classical upper limit rate (green line) is computed without taking into account any uncertainties of resonance energies and strengths.

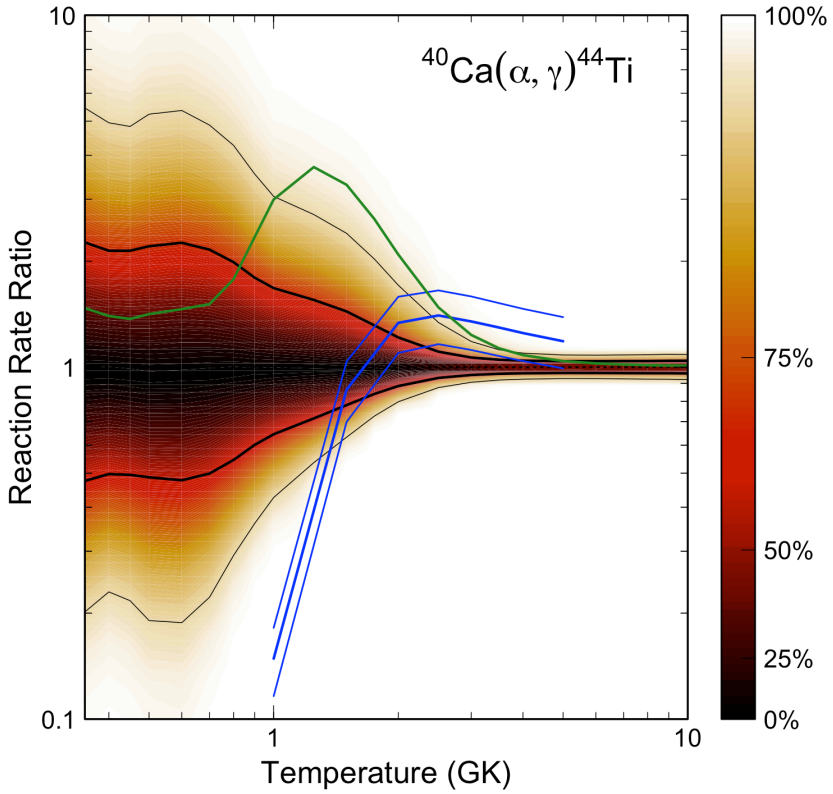

FIG. 6. (Color online) Reaction rates for ^{40}Ca(α,γ)^{44}Ti; for a better comparison, all rates are normalized to the present recommended (median) Monte Carlo rate. Red: contour plot of Monte Carlo based rates; the shading indicates the coverage probability in percent (legend on right-hand side); for example, the thick (thin) black lines indicate the high and low Monte Carlo rates for a coverage probability of 68% (95%). Blue: previously reported "upper limit", "complete rate" and "lower limit" from Ref. [45]; the latter work did not take into account any of the unobserved resonances and only presents rates between 1.0 GK and 5.5 GK. Green: classical "upper limit" rate obtained if maximum contribution of $E_\alpha^{c.m.} = 2373$ keV ($E_x = 7500$ keV) is adopted (i.e., assuming a spectroscopic factor of unity).

For α-particles, we analyzed 11 level sequences in the $A = 28-40$ range and find that the extracted mean reduced width values depend only weakly on mass number. If we combine all level sequences, regardless of mass number, A, and spin-parity, J^π, into one set, a value of $\langle\theta_\alpha^2\rangle = 0.018 \pm 0.002$ is found. This value is about a factor of 2 higher than the result reported previously [10], which was based on a subset of the full (p,α) data set analyzed here.

Mean proton reduced widths are extracted for 33 level sequences in the $A = 34-67$ range. We find significant scatter in the mean values for different mass numbers and J^π values. For a given spin J, the $\langle\theta_p^2\rangle$ values scatter over up to an order of magnitude, depending on mass number. For $A \leq 40$ the mean reduced proton widths are higher, on average, compared to the $A > 40$ range. These results are important because they facilitate an improved random sampling of thermonuclear reaction rates: instead of using one *global* mean reduced proton width value for all mass numbers and spin-parities, our results allow for the first time to employ *local* values in the random sampling. Furthermore, the level sequences with the largest number of states ($\approx$200) are used to study the dependence of the mean proton reduced width on the excitation energy range. We find only small variations over a range of ≈ 1.6 MeV. Thus, the observed scatter of $\langle\theta_p^2\rangle$ values is unlikely to be caused by differences in excitation energy, but it presumably reflects inherent differences in the nuclear structure of the compound nuclei under consideration.

As an example for the application of the present results, we consider the thermonuclear rates of the ^{40}Ca(α,γ)^{44}Ti reaction. When applying the mean reduced α-particle width and associated uncertainty derived here to a particular unobserved low-energy resonance, the estimation of the reaction rates is significantly improved over previous results. Our new reaction rates may have an important impact on the final ^{44}Ti abundance in core-collapse supernovae.

ACKNOWLEDGMENTS

This work was supported in part by the National Science Foundation under award number AST-1008355 and the U.S. Department of Energy under Contract No. DE-FG02-

97ER41041, DE-FG02-97ER41042, and DE-NA0001784.

---

[1] C. E. Porter and R. G. Thomas, Phys. Rev. **104**, 483 (1956).

[2] O. Bohigas, M. J. Giannoni, and C. Schmit, Phys. Rev. Lett. **52**, 1 (1984).

[3] T. A. Brody, J. Flores, J. B. French, P. A. Mello, A. Pandey, and S. S. M. Wong, Rev. Mod. Phys. **53**, 385 (1981).

[4] H. A. Weidenmüller and G. E. Mitchell, Rev. Mod. Phys. **81**, 539 (2009).

[5] P. Koehler, F. Bečvář, M. Krtička, J. Harvey, and K. Guber, Physical Review Letters **105** (2010).

[6] H. A. Weidenmüller, Phys. Rev. Lett. **105**, 232501 (2010).

[7] P. E. Koehler, Phys. Rev. C **84**, 034312 (2011).

[8] J. F. Shriner, Jr, H. A. Weidenmüller, and G. E. Mitchell, "Data on neutron widths do not refute random–matrix theory," (2012), arXiv:1209.2439.

[9] E. S. Reich, Nature **466**, 1034 (2010).

[10] R. Longland, C. Iliadis, A. Champagne, J. Newton, C. Ugalde, A. Coc, and R. Fitzgerald, Nuclear Physics A **841**, 1 (2010).

[11] A. M. Lane and R. G. Thomas, Rev. Mod. Phys. **30**, 257 (1958).

[12] C. Iliadis, R. Longland, A. Champagne, A. Coc, and R. Fitzgerald, Nuclear Physics A **841**, 31 (2010).

[13] C. Iliadis, R. Longland, A. Champagne, and A. Coc, Nuclear Physics A **841**, 323 (2010).

[14] J. M. Blatt and V. F. Weisskopf, *Theoretical Nuclear Physics* (John Wiley and Sons, New York, 1952).

[15] F. H. Fröhner, *Nuclear Theory and Applications*, IAEA-SMR-43 (1980) p. 59.

[16] F. James and M. Roos, Computer Physics Communications **10**, 343 (1975).

[17] G. Cowan, *Statistical Data Analysis*, Oxford Science Publications (Clarendon Press, New York, 1998).

[18] `http://www.tunl.duke.edu/nucldata/Theses/TUNL_Theses.shtml`.

[19] D. L. Sellin, *Excited States in* ^{19}F, Ph.D. thesis, Duke University (1969), unpublished.

[20] E. Bilpuch, A. Lane, G. Mitchell, and J. Moses, Physics Reports **28**, 145 (1976).

[21] J. M. Drake, E. G. Bilpuch, G. E. Mitchell, and J. F. Shriner, Phys. Rev. C **49**, 411 (1994).

[22] R. O. Nelson, *Proton Resonance Spectroscopy in* ^{28}Si *and* ^{30}P, Ph.D. thesis, Duke University (1983).

[23] D. Fang, *Proton Resonance Spectroscopy in* ^{32}S, Ph.D. thesis, Triangle Universities Nuclear Laboratory, Fudan University (1987).

[24] J. William K. Brooks, *Proton Resonance Spectroscopy in* ^{36}Ar, Ph.D. thesis, Duke University (1988).

[25] B. J. Warthen, *Proton Resonance Spectroscopy in* ^{40}Ca, Ph.D. thesis, Duke University (1987).

[26] J. S. Bull, *Entrance Channel Correlations in* ^{40}Ca, Ph.D. thesis, Duke University (1989).

[27] J. R. Vanhoy, E. G. Bilpuch, C. R. Westerfeldt, and G. E. Mitchell, Phys. Rev. C **40**, 1959 (1989).

[28] W. M. Wilson, Jr., *A High-Resolution Study of Proton Resonances in* ^{41}Sc*,* ^{43}Sc*, and* ^{45}Sc, Ph.D. thesis, Duke University (1973).

[29] B. W. Smith, *Level Density Studies in* ^{45}Sc, Ph.D. thesis, Duke University (1989).

[30] S. J. Lokitz, *A High Resolution Study of* p + ^{44}Ca *Reactions*, Ph.D. thesis, North Carolina State University (2004).

[31] N. H. Prochnow, *A High-Resolution Study of Proton Resonances in* ^{47}V*,* ^{49}V*, and* ^{51}V, Ph.D. thesis, Duke University (1971).

[32] J. Li, *Level Density Studies in* ^{49}V, Ph.D. thesis, Duke University (1990).

[33] W. C. Beal, Jr., *A High-Resolution Study of Proton Resonances in* ^{51}Mn, Ph.D. thesis, North Carolina State University (2004).

[34] M. S. L. K. McLean, *A High-Resolution Study of the* ^{52}Cr$(\mathrm{p},\mathrm{p}_0)$ *and* ^{52}Cr$(\mathrm{p},\mathrm{p}_1)$ *reactions*, Ph.D. thesis, North Carolina State University (2005).

[35] J. D. Moses, *A High Resolution Study of Isobaric Analog Resonances in* ^{51}Mn*,* ^{53}Mn*, and* ^{55}Mn, Ph.D. thesis, Duke University (1970).

[36] D. S. Flynn, *A High-Resolution Study of Proton Resonances in* ^{55}Co*,* ^{59}Cu*, and* ^{61}Cu, Ph.D. thesis, Duke University (1976).

[37] W. A. Watson, III, *A High Resolution Study of Proton Resonances in* ^{57}Co, Ph.D. thesis, Duke University (1980).

[38] K. B. Sales, *A High Resolution Study of Proton Resonances in* ^{65}Ga *and* ^{67}Ga, Ph.D. thesis, North Carolina State University (1980).

[39] P. A. Young, C. L. Fryer, A. Hungerford, D. Arnett, G. Rockefeller, F. X. Timmes, B. Voit,

C. Meakin, and K. A. Eriksen, The Astrophysical Journal **640**, 891 (2006).

[40] S. A. Grebenev, A. A. Lutovinov, S. S. Tsygankov, and C. Winkler, Nature **490**, 373 (2012).

[41] E. Zinner, Annu. Rev. Earth Planet. Sci. **26**, 147 (1998).

[42] E. L. Cooperman, M. H. Shapiro, and H. Winkler, Nucl. Phys. A **284**, 163 (1977).

[43] P. M. Endt, Nuclear Physics A **521**, 1 (1990).

[44] C. Vockenhuber, C. O. Ouellet, L. S. The, L. Buchmann, J. Caggiano, A. A. Chen, H. Crawford, J. M. D'Auria, B. Davids, L. Fogarty, D. Frekers, A. Hussein, D. A. Hutcheon, W. Kutschera, A. M. Laird, R. Lewis, E. O'Connor, D. Ottewell, M. Paul, M. M. Pavan, J. Pearson, C. Ruiz, G. Ruprecht, M. Trinczek, B. Wales, and A. Wallner, Phys. Rev. C **76**, 035801 (2007).

[45] D. Robertson, J. Görres, P. Collon, M. Wiescher, and H. W. Becker, Phys. Rev. C **85**, 045810 (2012).

[46] J. Chen, B. Singh, and J. A. Cameron, Nuclear Data Sheets **112**, 2357 (2011).

[47] P. Guazzoni, M. Jaskola, L. Zetta, K. Chong-Yeal, T. Udagawa, and G. Bohlen, Nucl. Phys. A **564**, 425 (1993).

[48] T. Yamaya, K. Ishigaki, H. Ishiyama, T. Suehiro, S. Kato, M. Fujiwara, K. Katori, M. H. Tanaka, S. Kubono, V. Guimaraes, and S. Ohkubo, Phys. Rev. C **53**, 131 (1996).